Available online at www.sciencedirect.com
ScienceDirect
International Journal of Pharmaceutics 340 (2007) 153–162
INTERNATIONAL JOURNAL OF PHARMACEUTICS
www.elsevier.com/locate/ijpharm

Pharmaceutical nanotechnology

Solid lipid nanoparticles loaded with insulin by sodium cholate-phosphatidylcholine-based mixed micelles: Preparation and characterization

Jie Liu, Tao Gong, Changguang Wang, Zhirong Zhong, Zhirong Zhang *

Key Laboratory of Drug Targeting, Ministry of Education, Sichuan University, No. 17, Section 3, Southern Renmin Road, Chengdu, Sichuan 610041, PR China

Received 9 December 2006; received in revised form 10 February 2007; accepted 7 March 2007
Available online 12 March 2007

Abstract

Solid lipid nanoparticles (SLNs) loaded with insulin-mixed micelles (Ins-MMs) were prepared by a novel reverse micelle-double emulsion method, in which sodium cholate (SC) and soybean phosphatidylcholine (SPC) were employed to improve the liposolubility of insulin, and the mixture of stearic acid and palmitic acid were employed to prepare insulin loaded solid lipid nanoparticles (Ins-MM-SLNs). Some of the formulation parameters were optimized to obtain high quality nanoparticles. The particle size and zeta potential measured by photon correlation spectroscopy (PCS) were 114.7 ± 4.68 nm and -51.36 ± 2.04 mV, respectively. Nanospheres observed by transmission electron microscopy (TEM) and scanning electron microscopy (SEM) showed extremely spherical shape. The entrapment efficiency (EE%) and drug loading capacity (DL%) determined with high performance liquid chromatogram (HPLC) by modified ultracentrifuge method were $97.78 \pm 0.37\%$ and $18.92 \pm 0.07\%$, respectively. Differential scanning calorimetry (DSC) of Ins-MM-SLNs indicated no tendency of recrystallisation. The core-shell drug loading pattern of the SLNs was confirmed by fluorescence spectra and polyacrylamide gel electrophoresis (PAGE) which also proved the integrity of insulin after being incorporated into lipid carrier. The drug release behavior was studied by in situ and externally sink method and the release pattern of drug was found to follow Weibull and Higuchi equations. Results of stability evaluation showed a relatively long-term stability after storage at 4 °C for 6 months. In conclusion, SLNs with small particle size, excellent physical stability, high entrapment efficiency, good loading capacity for protein drug can be produced by this novel reverse micelle-double emulsion method in present study.

Keywords: Insulin; Solid lipid nanoparticle; Mixed micelle; Double emulsion; Recrystallisation; Drug loading pattern

1. Introduction

Recently, with the advancement in biotechnology, efficient delivery of peptides or proteins has attracted considerable attention and interest (Barichello et al., 1999). However, most of the protein and peptide drugs used in therapeutics are administered by parenteral routes, which are poorly accepted by patients.

It is especially true in the case of insulin, a polypeptide widely applied to treat diabetes mellitus in clinic. Great efforts have been made to improve the existing parenteral dosage forms to increase patient compliance since 1923 (Gómez-Pérez and Rull, 2005). Despite the significant developments made in insulin therapy over the past 60 years, non-invasive insulin delivery remains an elusive goal (Pillai and Panchagnula, 2001). Insulin is the only molecule to have attracted so much attention from drug delivery scientists, therefore, it is not surprising that almost all possible routes (Trehan and Agsar, 1998) and numerous delivery systems such as liposomes (Zhang et al., 2005), nanoparticles (Cui et al., 2006), microemulsions (Çilek et al., 2005) and self-regulated insulin delivery systems (Zhang and Wu, 2004) have been explored for insulin delivery to achieve this goal.

Among the promising approaches towards developing non-invasive insulin delivery systems, use of nanoparticles seems to be an effective strategy. Nanoparticles have recently been proposed as valuable vehicles for efficient drug transport to the biomembranes while avoiding unwanted phagocytic mechanisms (Schurch et al., 1990; Makino et al., 2003) and adverse degradation of protein drugs. However, the cytotoxicity of the

* Corresponding author. Tel.: +86 28 85501566; fax: +86 28 85501615.
E-mail address: zrzzl@vip.sina.com (Z. Zhang).

0378-5173/$ – see front matter © 2007 Elsevier B.V. All rights reserved.
doi:10.1016/j.ijpharm.2007.03.009

polymers after internalization into cells is a crucial and often discussed aspect (Smith and Hunneyball, 1986). Therefore, increasing attention has been focused on SLNs, which derive from physiological compatible lipids represent novel safe and effective alternatives for conventional polymeric nanoparticles by adopting their advantages (Wang et al., 2002) and avoiding their potential toxicities (Müller et al., 1997).

Despite of the encouraging potential applications of biocompatiable SLNs, formulation of watersoluble peptide drugs involving these carriers still remains a challenge. Such potential challenges come from the inherent unwanted properties of proteins (poor solubility, easy denaturation during preparation course, and short half-life) (Müller and Keck, 2004) and the particular difficulties in incorporating and dispersing of hydrophilic drugs into the lipid cores of nanoparticles with high drug loading efficiency. These obstacles hinder the further application of lipid nanospheres in vivo.

Among the present encapsulation methods, the high pressure homogenization (HPH) has been generally recognized as a reliable and powerful technique for the preparation of SLNs (Mehnert and Mäder, 2001). Nevertheless, the drugs are susceptible to high shear stress and are destroyed during the formulation process (Perez et al., 2002). Preparation via microemulsion is another preferred way to produce SLNs, however, the required high temperature (60–70 °C) will result in the destabilization of the labile drug. In addition, it has to be remarked critically, that high concentrations of surfactants and cosurfactants are necessary for formulating purposes, which is less desirable with respect to regulatory purposes and application. In contrast, w/o/w method represents a relatively simple and efficient way to prepare SLNs loaded with instable and hydrophilic drugs (Morel et al., 1998). However, the average size is often in the micrometer range without restrict control of formulation parameters (Cortesi et al., 2002), and the drug loading capacity of the carriers is reduced markedly due to the rapid migration and, therefore, loss of drug into the external aqueous phase.

Hence, the main aim of this work was to formulate hydrophilic peptide drugs into SLNs by a reverse micelle-double emulsion strategy to produce enhanced drug entrapment efficiency, drug loading efficacy and sustained release behavior without "burst effect". In a previous report, Cui et al. (2006) and her group have developed a novel reverse micelle-solvent evaporation method to prepare polymeric nanoparticles loaded with insulin-phospholipid complex which showed some preferred properties. And in our study, a novel reverse micelle-double emulsion strategy was employed to produce SLNs loaded with insulin. Porcine insulin was used as a model drug due to its water solubility and typical property of proteins. SC and SPC were applied as solubilizers and stabilizing agents. Initially, insulin was solubilized into the mixed reverse micelles constituted by SC and SPC. A combination of stearic acid and palmatic acid was used as biocompatible lipid matrix, which can form imperfect crystals, and hopefully to accommodate more micelles and prevent expulsion of drugs during storage thus enhance the shelf-life of insulin. Some of the formulation parameters were investigated to figure out if they are crucial and restrictive for the encapsulation of insulin into the oily core of the nanoparticles. Thus, nanocarriers with some expectable properties such as high drug loading ability and entrapment efficiency can be produced through the optimized formulation. Following that, the physicochemical characteristics and in vitro release behavior of the nanoparticles were also evaluated, which can provide some useful and essential information for in vivo studies. And from the preliminary studies, SLNs loaded with insulin based on mixed micelles appear to be a good candidate for invasive insulin delivery.

2. Materials and methods

2.1. Materials

Pure crystalline porcine insulin was purchased from Xuzhou Wanbang Bio-Chemical Co. Ltd. (No. 0312A02, Jiangsu, China), with a nominal activity of 28 IU mg^{-1}. Stearic acid (obtained from Shanghai Chemical Reagent Co. Ltd., China) and palmitic acid (obtained from Chengdu Kelong Chemical Plant, China) were used as lipid materials of SLNs. Soybean phosphatidylcholine (purchased from Shanghai Taiwei Pharmaceutical Co. Ltd., China) and sodium cholate (supplied by Beijing Aoboxing Biotechnologies Co. Ltd., China) were used to form mixed reverse micelles while poloxamer 188 (from Nanjing Weier Chemical Co. Ltd., China) was employed as emulsifier. Double distilled water was used for all solutions and dilution. All the other reagents were of analytical grade and used without further purification.

2.2. Preparation of Ins-MM-SLNs

Ins-MM-SLNs were prepared by reverse micelle-double emulsion technique. Typically, an insulin solution was prepared as follows: a weighted amount of insulin was dissolved in 0.05 M sodium hydroxide solution, 0.1 M hydrochloric acid was then added and the solution was completed to a final volume of 5 ml with water. The pH of this solution was 3 and the maximum concentration could reach 30 mg/ml. Different amount of SC was added into 200 μl of previously prepared insulin solution (inner aqueous phase), and then, the solution was added to a 1 ml ethyl acetate solution containing 1mg mixture of stearic acid and palmitic acid (1:1, w/w) and different amount of SPC (oily phase). This mixture was dispersed with an ultrasonic probe (JY92-II ultrasonic processor, Ningbo Scientz Biotechnology Co. Ltd., China) for 15 s at 40 W leading to a primary W/O emulsion. A double emulsion W/O/W was formed after addition of 4 ml of poloxamer 188 solution of different concentration or different pH values (outer aqueous phase) to the previous W/O emulsion followed by sonication for 15 s at 80 W. This double emulsion was then diluted to 10 ml with previously mentioned poloxamer 188 solution. The organic solvent was evaporated for 3h in a rotary evaporator (Büchi, R-144 rotavaporator, Switzerland) at 25 °C. The influence of variables such as amount of SC, SC to SPC ratios and pH values of the outer aqueous phase as well as concentration of poloxamer 188 on the entrapment efficiency and drug loading of nanoparticle suspensions was investigated.

One hundred and fifty milligrams of sucrose was dissolved in 1 ml Ins-MM-SLNs suspension. The mixture was stored at −40 °C for 4h and then lyophilized under vacuum for 24 h.

2.3. Transmission electron microscopy (TEM)

The morphology of the Ins-MM-SLNs was examined by TEM (H-600, Hitachi, Japan). Before analysis, the samples were diluted 1:2 and stained with 2% (w/v) phosphotungstic acid for 30 s and placed on copper grids with films for observation.

2.4. Scanning electron microscopy (SEM)

In order to verify the result of TEM, the morphology of Ins-MM-SLNs was viewed using a conventional scanning electron microscope (JSM-5900LV, JEOL, Japan) at an accelerating voltage of 20 kV. One drop of the nanoparticle suspension was placed on a graphite surface. After oven-drying, the sample was coated with gold using an Ion Sputter.

2.5. Photon correlation spectroscopy

The average diameter and polydispersity index of Ins-MM-SLNs were measured by photon correlation spectroscopy (PCS) (Malvern zetasizer Nano ZS90, Malvern instruments Ltd., UK) with a 50 mV laser. Typically, 0.2 ml of Ins-MM-SLNs was diluted by 1 ml of water before adding into the sample cell. The measurements were performed at 25 °C at a fixed angel of 90°. The measurement time was 2 min and each run underwent 10 subruns. Each value reported is the average of at least three measurements. The polydispersity index can reflect the size distribution of nanosphere population.

2.6. Determination of zeta potential

The electrophoretic mobility and zeta potential of the lipid carriers were measured by Malvern zetasizer Nano ZS90 (Malvern instruments Ltd., UK). Before the measurements, the Ins-MM-SLNs samples were diluted with 1:5. Each sample was analyzed in triplicate, and the zeta potential values were calculated according to Smolochowski equation.

2.7. Differential scanning calorimetry (DSC)

DSC was performed with an EXSTAR 6000 thermogravimetric analyzer (EIKO, Japan). Insulin, the physical mixture of stearic acid and palmitic acid bulk material (1:1, w/w) and SLNs with or without insulin obtained by lyophilization were placed in conventional aluminium pans (about 10 mg) and a scan speed of 5 °C/min were employed.

The recrystallization index (RI) was calculated as follows (Eq. (1)) (Freitas and Müller, 1999):

$$\mathrm{RI}\,(\%) = \frac{\mathrm{Enthalpy}_{\mathrm{SLN\ dispersion\,(mJ/mg)}}}{\mathrm{Enthalpy}_{\mathrm{bulk\ materials\,(mJ/mg)}} \times \mathrm{Concentration}_{\mathrm{lipid\ phase\,(\%)}}} \times 100 \quad (1)$$

2.8. Entrapment efficiency (EE%) and drug loading (DL%)

For the quantitative determination of insulin, a reverse phase HPLC method was used (Waters 2690 separation module and a 996 Photodiode Array (PDA) detector, Inertsil ODS-3 column 150 mm × 4.6 mm, 5 μm). The mobile phase was a premixed isocratic mixture of 0.2 M sodium sulfate anhydrous solution adjusted to pH 2.3 with phosphoric acid and acetonitrile (72:28, v/v). The injection volume for samples and standards were 20 μl and eluted at a flow rate of 1.0 ml min^{-1} at 40 °C. The eluent was monitored at 214 nm (AUFS = 1) (Xu et al., 2006).

The amount of insulin loaded into the SLNs was determined as follows: 0.4 ml of 0.1 M hydrochloric acid was added to 0.6 ml of freshly prepared Ins-MM-SLNs suspension (equal to 60 μg insulin), and the mixture was ultracentrifuged for 15 min at 4 °C at 14,000 rpm (Allegra X-22R Centrifuge, F2402H rotor, Beckman Coulter Inc., CA, USA) in order to isolate the entrapped insulin from the unentrapped insulin. Then, the supernatant was removed and nanoparticle sediments washed by distilled water (adjusted to pH 3.0 with Hydrochloric acid) in triplicate were dissolved in 200 μl mobile phase, then the mixture for further HPLC analysis was vortexed till it became totally clear. The entrapment efficiency (EE) of insulin in SLNs was also determined using the following Eq. (2):

$$\mathrm{EE}\,(\%) = \frac{\text{amount of drug in precipitations}}{\text{amount of drug added}} \times 100 \quad (2)$$

Drug loading was calculated as drug analyzed in the nanoparticles versus the total amount of the drug and the excipients added (lipid, SPC, SC and poloxamer188) during preparation according to Eq. (3):

$$\mathrm{DL}\,(\%) = \frac{\text{amount of drug in precipitations}}{\text{amount of drug added+amount of excipent added}} \times 100 \quad (3)$$

2.9. In vitro release

2.9.1. In situ release method

Release experiments were performed by suspending a weighed amount of freeze-dried Ins-MM-SLNs (equal to insulin 1 mg) in 50 ml, pH 7.4 phosphate buffer solution containing 1.5% (w/w) glycine as stabilizer. During the experiment (144 h), samples were shaken horizontally in a constant temperature shaker (Shenzhen worldwide industry, Co. Ltd., China) at 37 ± 1 °C and 60 strokes per minute. At scheduled time intervals, 0.6 ml of the sample was removed and replaced with 0.6 ml fresh release medium. 0.4 ml 0.1 M hydrochloric acid was added into the withdraw sample, and the mixture was ultracentrifuged for 15 min at 4 °C at 14,000 rpm, then the supernatant was collected and stored at −80 °C. Samples were analyzed by RP-HPLC and the amount of insulin in the supernatant was calculated by means of a calibration curve.

2.9.2. Externally sink release method

Ins-MM-SLNs were subjected to in vitro release studies in externally sink condition. Lyophilized nanoparticles (equivalent

to 0.1 mg drug) were placed into centrifuge tubes containing 1.2 ml of dissolution media and shaken in a horizontal shaker (Shenzhen worldwide industry, Co. Ltd., China) (60 rpm) at 37 ± 1 °C. The dissolution media was pH 7.4 phosphate buffer solution with 1.5% (w/w) glycine. At predetermined time intervals, 0.8 ml 0.1 M hydrochloric acid was added, the supernatant was collected and stored at −80 °C after centrifugation of the mixture (14,000 rpm, 15 min, 4 °C) and the sediments was replaced by 1.2 ml fresh medium. The amount of drug released from the nanoparticles was analyzed using HPLC as described above.

2.10. Polyacrylamide gel electrophoresis (PAGE)

The integrity of insulin following entrapment in SLNs and the protein loading patterns were investigated by polyacrylamide gel electrophoresis (Wu and Ping, 2003). Different concentration of freshly prepared SLN samples, native insulin solutions, native insulin solutions added with Zn^{2+} and lyophilized Ins-MM-SLNs redispersed with distilled water were loaded onto a vertical slab gel consisting of 8% separating gel and 5% stacking gel and subjected to electrophoresis at 100 mV. Following electrophoresis the gels were stained with Coomassie brilliant Blue (0.1%, w/v) (Sigma, USA) in water:methanol:acetic acid (45:45:10, v/v/v) to visualize the protein.

2.11. Fluorescence spectrum

Insulin solution, freshly prepared blank SLNs, Ins-MMs and Ins-MM-SLNs were estimated to prove the potential of micelles core-shell type nanoparticle formation by the measurement of fluorescence spectroscopy (Shimadzu RF-5301 spectrofluorometer, Shimadzu Co. Ltd., Japan). Excitation wavelength was 250 nm for emission spectra, and the scanning range was from 250 to 650 nm. Excitation and emission bandwidths were 5 and 5 nm, respectively.

2.12. Stability studies

Three batches of SLNs were stored at 4 °C for 6 months, average size and entrapment efficiency were determined at 0, 10, 30, 60, 90, 120 and 180 days after prepared. Each sample was detected for three times.

3. Results and discussion

In order to optimize the Ins-MM-SLNs preparation by the reverse micelle-double emulsion method, different process variables were evaluated. After preliminary trials, the mixture of stearic acid and palmitic acid (1:1) which produced high entrapment efficiency were considered for the study.

The use of bile salts (cholate salts) (Müller et al., 1996; Siekmann and Westesen, 1992; Fuentes et al., 2002; Young et al., 2003) or phosphatidylcholine (Fuentes et al., 2005; Mei et al., 2003; Sznitowska et al., 2001; Yang et al., 1999) in the preparation of nanoparticles has been widely reported. And there were some reports about increasing drug solubility by means of

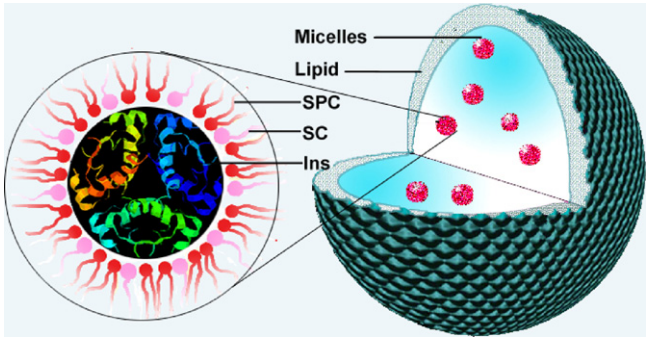

Fig. 1. Schematic representation of the structure of Ins-MM-SLNs.

bile salt-phosphatidylcholine-based mixed micelles. However, no reports have been concerned with the application in preparation of nanoparticles. In the present study, sodium cholate played double roles as both solubilizer and emulisifier. Reverse micelles of SC and SPC were formed in organic phase, which were confirmed by the red shift of fluorescence emission peaks of insulin (from 304 to 310 nm) (Yamamoto et al., 2007) and average size determined by PCS (about 30 nm), which suggested the formation of micelles. Fig. 1 is a schematic diagram which represents the proposed structure of the Ins-MM-SLNs. The long alkyl chains of lipid were twisted with the hydrophobic chains of SPC and SC. A continuous shell was formed by the polar head groups of lipids, which was confirmed by the disappearance of fluorescence maximum of insulin (304 nm).

3.1. Influence of sodium cholate

The influence of SC amounts on the size, entrapment efficiency of nanoparticles was described in Fig. 2. Increase in surfactant concentration till 0.05% (w/v) resulted in significant reduction in size and enhancement of entrapment efficiency of nanoparticles, and a further increase did not have much influence on the particle size and the entrapment efficiency. The decrease in size of nanoparticles at high surfactant concentrations is due to effective reduction in interfacial tension between the aqueous and lipid phases leading to the formation of emulsion droplets of smaller size. High surfactant concentrations effectively stabilized the particles by forming a steric barrier on the particle surface and thereby protect the particles from coagulation. By increasing the concentration of SC, the solubilization

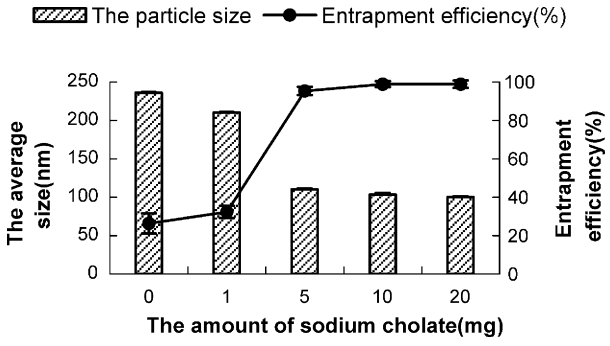

Fig. 2. Influence of the concentration of SC solution on the mean diameter and entrapment efficiency of lipid nanoparticles.

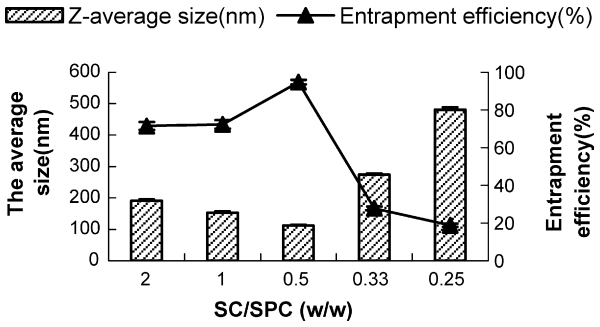

Fig. 3. Influence of the SC/SPC ratio on the average diameter and entrapment efficiency of lipid nanoparticles.

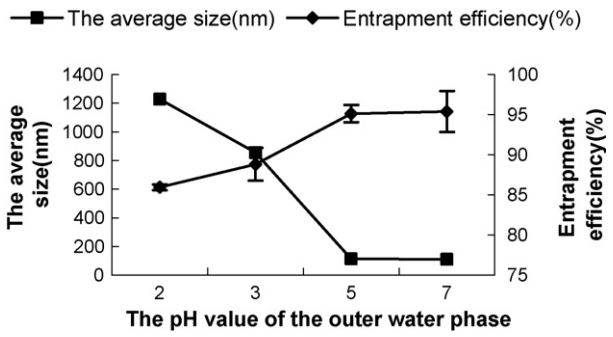

Fig. 4. Influence of the pH value of the outer water phase on the mean diameter and entrapment efficiency of lipid nanoparticles.

of mixed micelle increased, which resulted in the high entrapment efficiency of nanoparticles. Nevertheless, further increase of surfactant amount did not lead to the enhancement of incorporation efficacy because the highest affinity between insulin and MMs was achieved when 0.05% (w/v) was employed. The optimum concentration of SC to produce smaller sized nanoparticles (103.4 ± 2 nm) was 0.1% (w/v), and the entrapment efficiency is $98.92 \pm 1.5\%$. Slight differences in size and entrapment efficiency of resulted SLNs were found when 0.05% and 0.1% of SC were employed, so 0.05% SC was adopted for the further investigations for some safety considerations.

3.2. Influence of SC/SPC ratio

The influence of SC/SPC ratio on the entrapment efficiency and average size of Ins-MM-SLNs is shown in Fig. 3. Initially, increasing of SPC fraction was accompanied by an increasing affinity of the drug to MM, however, further increase in the SPC fraction showed relatively lower affinity to MM. The SC/SPC of 1:2 seemed to be a turning point, which exhibited the highest affinity of insulin to MM and resulted in the highest entrapment efficiency and narrowest size distribution of Ins-MM-SLNs.

It appears that presence of the planar aromatic rings (Hammad and Müller, 1998), i.e. Phe (Phe-A1, -A25, -A26) and Tyr residues (Tyr-A14, -A19, -B16, -B26, -B27) in the case of insulin facilitate the interaction of the drug molecule with the lipophilic part of the micelles by insertion between the molecules of the surfactants. Such interaction of deep penetration is expected to increase as the lipophilic part of the MM is increased by increasing the SPC fraction. However, further increase of SPC amount would result in highly-reduced solubility of insulin and entrapment efficiency of insulin loaded nanoparticles, because the presence of hydrophilic groups of insulin greatly limits the interaction with the lipophilic part of SC/SPC-MMs.

3.3. Influence of poloxamer 188(F68) concentration

The choice of the stabilizers and their concentration is of great impact on the quality of the SLN dispersion. So, the influence of the stabilizer concentration on the particle size and entrapment efficiency was also investigated. It was possible to form Ins-MM-SLNs using 0 and 5% F68 concentrations. Table 1 clearly shows that the increase of the stabilizer concentration significantly increase entrapment efficiency, but has little influence on the reduction of the droplet size. It seems contradictory to some previous findings. As it is generally recognized that high concentrations of the stabilizer can reduce the surface tension and facilitate the particle partition during the size reduction process. The possible explanation of this result is that the increase of the surface area during first ultrasonic process occurs much more rapidly than the second ultrasonic process. In other words, the primary dispersion must contain excessive emulsifier or stabilizer molecules, which can rapidly cover the new generated surfaces (Mehnert and Mäder, 2001). In this case, SC played the part to compete with the agglomeration of uncovered lipid surfaces and once the optimum packing of the stabilizer and the minimum droplet size has been reached, higher concentrations of the stabilizer will not play any further role on particle size. So, poloxamer 188 had little influence on the reduction of particle size. However, the addition of poloxamer 188 can increase the viscosity of the external phase, reducing the diffusion speed of the drug and therefore increasing the entrapment efficiency of SLNs.

3.4. Influence of the pH value of external phase

In order to provide information about the nature of interaction between the lipids and MMs, studies were subsequently carried out using external phase with different pH values. Fig. 4

Table 1
Influence of the concentration of F68 solution on the mean size, PDI and entrapment efficiency of Ins-MM-SLNs ($n = 3$)

Poloxamer188 concentration (w/v%)	Mean size ± S.D.	PDI ± S.D.	Entrapment efficiency (%) ± S.D.
0	115.4 ± 0.9	0.178 ± 0.027	75.85 ± 2.45
0.1	109.7 ± 1.2	0.166 ± 0.021	99.71 ± 1.02
0.5	113.4 ± 0.7	0.217 ± 0.015	95.66 ± 3.23
1	106.2 ± 0.9	0.243 ± 0.011	95.38 ± 1.15
2	111.9 ± 1.0	0.155 ± 0.018	92.75 ± 2.89
5	112.5 ± 1.4	0.248 ± 0.024	85.94 ± 3.14

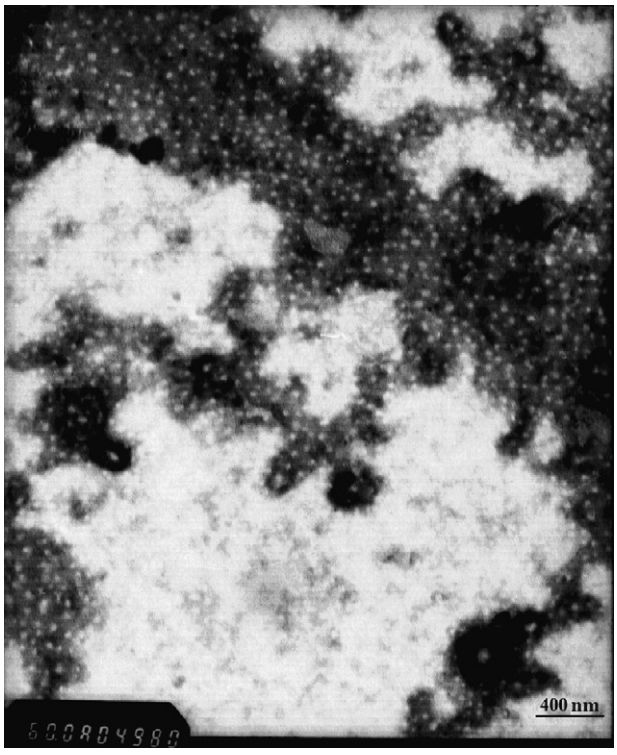

Fig. 5. Transmission electron micrograph of Ins-MM-SLNs, scale bar: 400 nm.

describes the influence of the pH conditions on the size and drug loading of the carriers. At pH conditions ranging from 2 to 7, the particle size decreased dramatically and their capacity to load the insulin increased as well. This fact can be attributed to the different surface charges of lipid particles in different circumstances. The lipid carrier displayed a more negative zeta potential (data not shown) in pH 7 than pH 2, and their capacity to entrap the MMs which were positively charged in internal phase of pH 3 was much higher. Furthermore, the decrease of zeta potential also led to the aggregation of the lipid spheres at lower pH, which resulted in the larger sizes of the particles under these conditions.

3.5. Particle morphology

Ins-MM-SLNs were characterized by PCS and exhibit a diameter of 114.7 ± 4.68 nm. The polydispersity index of 0.161 ± 0.021 indicates a narrow size distribution. The PCS results of three batches of lipid nanospheres are summarized in Table 2, which demonstrates that the preparation process is reproducible and stable.

TEM and SEM images of the SLNs are presented in Figs. 5 and 6, respectively. Both techniques confirm that the

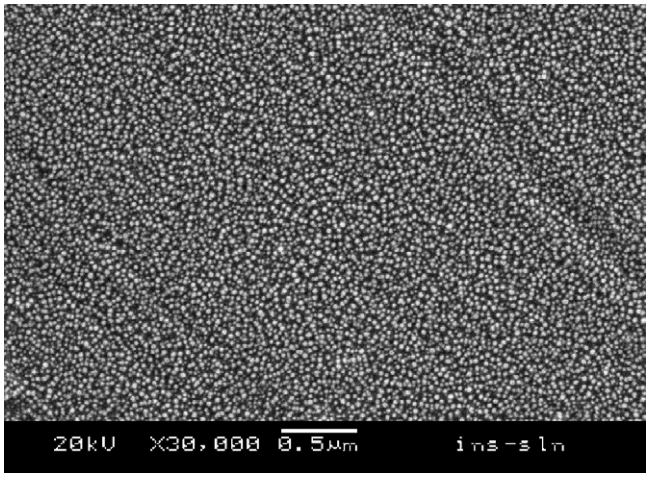

Fig. 6. Scanning electron micrograph of Ins-MM-SLNs, scale bar: 0.5 μm.

SLNs are circular in shape and well dispersed and separated on the surface.

The sizes of the SLNs determined by PCS did not agree well with TEM and SEM results. The diameter determined by PCS is 114.7 ± 4.68 nm, while determined by SEM and TEM are considerably smaller, about 50 and 60 nm, respectively. Though the results are quite different, it should be noted that these methods are based on totally different mechanisms and employing different sample preparation processes, which might lead to the discrepancy of the outcomes.

The size detection of Ins-MM-SLNs by PCS is carried out in aqueous state and in this case, lipid nanospheres are highly hydrated and the diameters detected by PCS are 'hydrated diameters', which are usually larger than their genuine diameters. And it should be mentioned, PCS does not 'measure' particle sizes (Mehnert and Mäder, 2001). Rather, it detects the fluctuations of light signals caused by the Brownian motion of the particles to calculate their sizes. Some of the uncertainties, for instance, may result from non-spherical particles since the particles are assumed ideally spherical in PCS calculation.

In the case of TEM sample preparation, Ins-MM-SLNs are stained with 2% (w/v) phosphotungstic acid and all the free water and even some of hydrated water was stained. This implies that the sizes of Ins-MM-SLNs derived from TEM might be considerably smaller than their real diameters.

For the SEM sample preparation, both the surface water and the water present in the SLN matrix are externally removed by oven-drying. Such drying apparently causes shrinkage so that the mean diameter determined by SEM is significantly smaller than that determined by PCS (Dubes et al., 2003).

Table 2
Particle size, polydispersity index, zeta potential, entrapment efficiency and drug loading of three batches of optimum formulation of Ins-MM-SLNs ($n = 3$)

Batch no.	Size (nm)	PDI	Zeta potential (mV)	Entrapment efficiency (%)	Drug loading (%)
1	109.7 ± 1.5	0.169 ± 0.025	−53.67 ± 0.81	97.81 ± 0.08	18.93 ± 0.015
2	115.7 ± 2.3	0.157 ± 0.027	−51.23 ± 0.50	98.11 ± 0.08	18.99 ± 0.015
3	119.0 ± 3.6	0.156 ± 0.018	−49.20 ± 0.89	97.43 ± 0.42	18.85 ± 0.084

3.6. Zeta potential

Zeta potential is a key factor to evaluate the stability of colloidal dispersion (Komatsu et al., 1995). In general, particles could be dispersed stably when absolute value of zeta potential was above 30 mV due to the electric repulsion between particles (Müller et al., 2000, 2001). As shown in Table 2, the average zeta potential of obtained SLN was about -51.36 ± 2.04 mV, and no trend was found for the zeta potential changes during storage. This demonstrates that the nanoparticles obtained in this study is a dynamic stable system.

3.7. DSC

DSC uses the fact that different lipid modifications possess different melting points and melting enthalpies (Mehnert and Mäder, 2001). It is a popular tool to investigate the crystallinity of colloidal SLN matrices. The DSC thermal behavior of the untreated lipid bulk was chosen as reference. Untreated mixture of stearic acid and palmitic acid showed a double endothermic peak upon heating with two maximums at 63.8 and 68.9 °C and an enthalpy of 219.4 mJ/mg (Table 3).

The crystallization behavior of freshly prepared blank-SLNs and Ins-MM-SLNs differs distinctly from the bulk lipid. The peaks of the DSC heating curves are broadened and the melting point is reduced to about 63.1 °C (Fig. 7, curve 'blank-SLN') and (Fig. 7, curve 'Ins-MM-SLNs'). In contrast to the untreated bulk, the melting points of colloidal systems were distinctly decreased by about 3 °C. According to Siekmann and Westesen (1994b), the melting point decrease of colloidal systems can be assigned to the colloidal dimensions of the particles in particular to their large surface to volume ratio and not to recrystallisation of the lipid matrices in a metastable polymorph possessing a lower melting point. The broadening of the heating peak and the reduction of the melting point indicate an increased number of lattice defects (Westesen et al., 1993). The small particle size and large surface being an energetically suboptimal state leads to a decrease of the crystallization point (Hunter, 1987).

It has been reported that the recrystallization index has an effect on the long-term stability of aqueous SLN dispersions (Mühlen, 1996). In general, dispersions with a highly recrystallized lipid phase (high recrystallization index) showed an accelerated growth in particle size. In other words, the SLNs with lower RIs present higher physical stability. Recrystallization indices higher than 100% were reported in gelled formulations (Siekmann, 1994a) and lower recrystallization indices often indicate that the fat fraction of SLNs is not externally solidified (Freitas and Müller, 1999), which infers a higher capacity. In the present study, the recrystallization index of blank SLNs and Ins-MM-SLNs were rather low, 27.78% and 17.73%, respectively (Table 3). Therefore, they showed good physical stability.

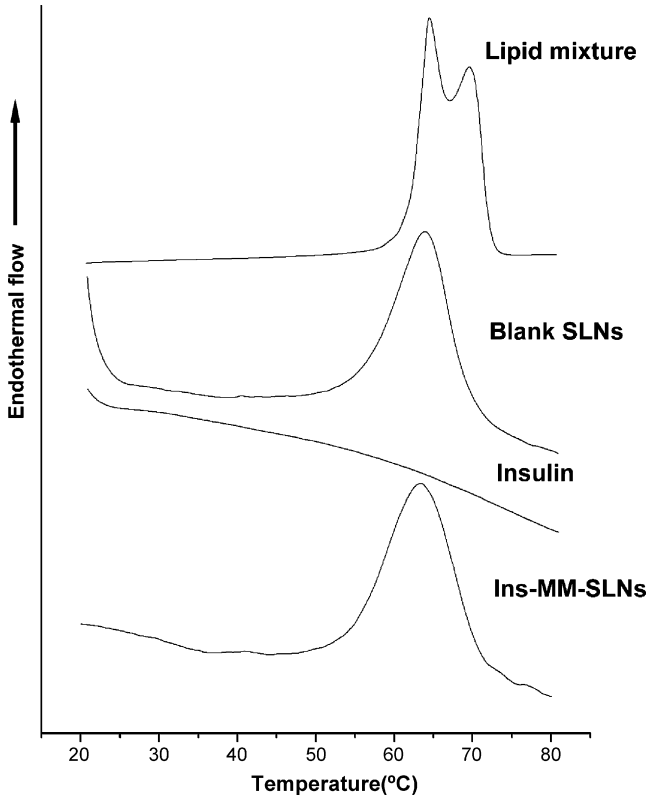

Fig. 7. Differential scanning calorimetry curves of bulk lipid mixture, insulin, solid lipid nanoparticles with and without insulin.

3.8. Entrapment efficiency (EE%) and drug loading (DL%)

The loading capacity of SLNs was found to be satisfactorily high, with an entrapment efficiency of $97.78 \pm 0.37\%$, and drug loading efficacy $18.92 \pm 0.07\%$. The extremely high incorpating rate may be attributed to the particular drug location patterns of the Ins-MM-SLNs. As mentioned above, the drug loading pattern was supposed to be a core-shell model, as is represented in Fig. 1. The solid lipid formed a spheric shell and insulin-contained mixed micelles of SC and SPC were dispersed in the solid matrix of the nanoparticle. By incorporating into the micelles, large hydrophilic molecules can be easily inserted into the lipid core.

Entrapment efficiency and drug loading of nanoparticles were determined using ultracentifugation with some modifications concerning with the specificity of the SLNs. Usually, due to the higher zeta potential of nanoparticles under aqueous dispersion with pH 6.0, the nanosized particles were difficult to

Table 3
Melting parameters and recrystallisation index (RI) of lipid mixture, blank-SLNs and Ins-MM-SLNs ($n = 3$)

	Enthalpy (mJ/mg)	Melting point (°C)	Peak width (°C)	RI (%)
Lipid mixture	219.40 ± 2.52	63.8 ± 1.5; 68.9 ± 1.2	25 ± 2	100
Blank-SLNs	43.88 ± 1.34	63.1 ± 1.1	30 ± 1	27.78 ± 0.53
Ins-MM-SLNs	28.05 ± 0.95	63.4 ± 1.6	28 ± 2	17.73 ± 0.40

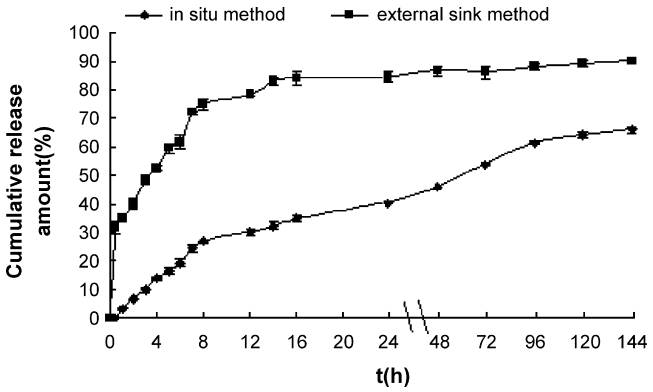

Fig. 8. In vitro release profiles of insulin from Ins-MM-SLNs in phosphate buffer solution (pH 7.4) by in situ and external sink methods ($n = 3$).

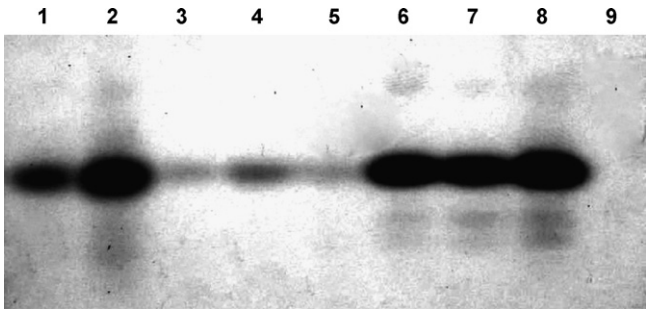

Fig. 9. Polyacrylamide gel electrophoresis analysis (8% separating gel and 5% stacking gel) of insulin, Ins-Zinc complexes and insulin loaded nanoparticles. Lanes: (1) insulin (1 mg/ml); (2) insulin (5 mg/ml); (3) Ins-MM-SLNs after washed; (4) unwashed Ins-MM-SLNs; (5) lyophilizated Ins-MM-SLNs; (6) Ins-$ZnSO_4$ complex;(7) Ins-$ZnCl_2$ complex; (8) insulin-10 mg; (9) control.

separate from dispersion by centrifugation. In order to separate the nanoparticles easily for further analysis, the pH value of nanoparticles dispersion was adjusted to 1.2 by addition of 0.1 M hydrochloric acid to reduce the zeta potential (the value was nearly zero in the system) and the nanoparticles can be easily separated by centrifugation (Hu et al., 2005).

3.9. Drug release of Ins-MM-SLNs

Fig. 8 illustrates in vitro release behaviors of Ins-MM-SLNs in two different release methods. For both methods, a biphasic drug release pattern was observed, that was a rapid drug release at the initial stage and followed by sustained release at a constant rate. No burst effect was observed, but the release rate of primary phase was considerably faster than the steady release phase. The possible explanation for the rapid release is that in the neutral medium with higher pH than the PI of insulin, the repulsion between insulin and SC-SPC-MMs would have occurred due to their identical charge, which may contribute to the broken down of micelles.

There were some differences between two methods. The initial drug release rate determined in situ was considerably lower than that obtained by the externally sink method. This might attribute to the higher concentration gradient in the latter. And it is worth to mention, due to the instability of insulin during incubation at 37 °C, the cumulative release amount from lipid nanospheres could never reach 100% in situ. In contrast, insulin exposed to a relatively stable environment in externally sink method. Additionally, the loosely bounded drug could be removed in the external sink conditions, while for in situ release, they could be absorbed on the surface of nanoparticles, and the absorbed amount might vary with the aggregation and disaggregation status of the particles. Thus, the result from externally sink method might simulate the in vivo release profile more properly. And the release data obtained from both methods were fitted into Weibull equation. Release of drug by in situ method followed Higuchi equation as well as Weibull equation.

3.10. PAGE

Proteins are characterized by their complex and well defined structures which have important implications regarding their biological activity. These molecules usually present problems related to instability and loss of activity during pharmaceutical formulation courses. The effect of excipients or formulation factors might influence the integrity of insulin. However, as shown in Fig. 9, no changes in the pattern of migration of insulin after being entrapped into lipid carriers either in freshly prepared sample or in lyophilizated form could be detected. The extra bands of higher and lower molecular weight shown in lanes of high concentration of insulin and insulin–zinc complex could be attributed to the presence of split or deamidated products and also some dimers or hexamers caused by high concentration or surplus of zinc ions. No additional bands were observed in Ins-MM-SLNs, suggesting that the integrity of the molecule was maintained after incorporation into lipid matrix. Further, the result also suggests that majority of insulin molecules was entrapped into lipid nanospheres according to the colors of the bands and the drug loading pattern might follows a drug enriched core-shell model (Müller et al., 2000).

3.11. Fluorescence spectrum

Further conclusive evidence of drug loading pattern of Ins-MM-SLNs was observed by fluorescence studies. Fluorescence emission intensity of insulin, Ins-MM-SLNs, blank SLNs and Ins-MMs is given in Fig. 10. Results from fluorescence spectroscopy studies clearly indicate that excitation at 250 nm, the maximum fluorescence wavelength of insulin solution is 304 nm due to the Tyr residue (Tyr-A14, -A19), whereas no such strong fluorescence intensity was detected in washed Ins-MM-SLNs or blank SLNs at 304 nm. A likely model for the interaction between SLNs and insulin involves concealing surface positional tyrosine within in lipid matrix. This study further convinced the core-shell formation of Ins-MM-SLNs.

3.12. Stability data

After 6 months storage at 4 °C, size of SLNs increased in the range from 115.57 ± 1.88 to 128.5 ± 2.4 nm. Entrapment efficiencies of Ins-MM-SLNs were lowered by 1.98% after 6 months of storage at 4 °C (Fig. 11). Transitions of lipid from metastable forms to stable form might occur slowly on storage

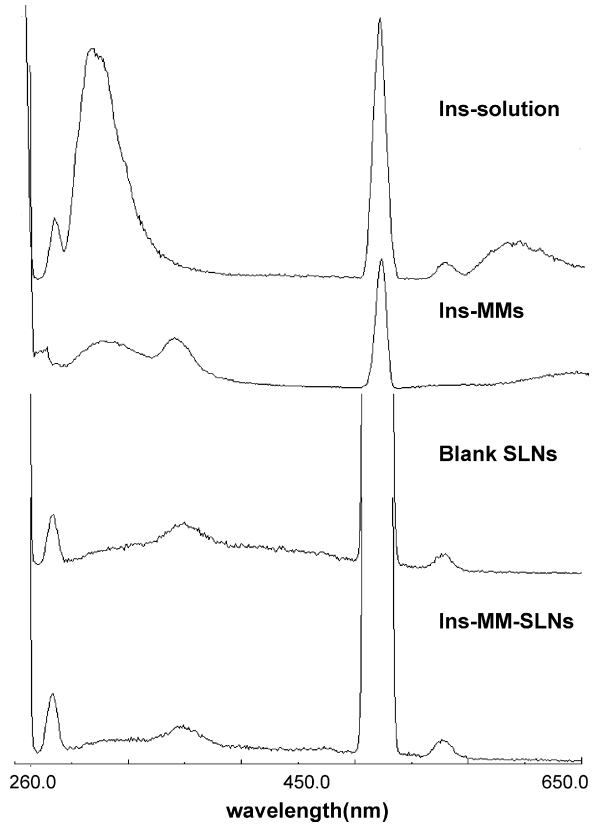

Fig. 10. Fluorescence absorption spectra of insulin, Ins-MMs, blank SLNs and Ins-MM-SLNs.

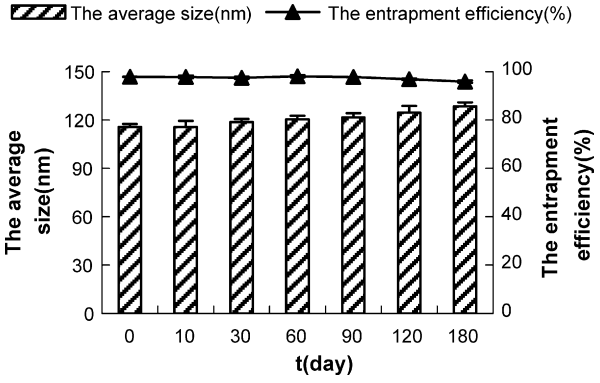

Fig. 11. Particle size and entrapment efficiency of Ins-MM-SLNs after 0, 10, 20, 30, 60, 90, 120 and 180 days of storage at 4 °C.

due to small particle size and the presence of emulsifier that may lead to drug expulsion from solid lipid nanoparticles (Mehnert and Mäder, 2001; Westesen et al., 1993; Westesen and Bunjes, 1995). However, the drug expulsion rate was slowed down dramatically due to the existence of reverse mixed micelles. Therefore the solid lipid nanoparticles prepared by reverse micelles-double emulsion method showed excellent storage stability.

4. Conclusions

In this paper, we have shown that a hydrophilic peptide, such as insulin, can be successfully formulated into solid lipid nanoparticles by formation of SC and SPC mixed micelles. Particles with a small size (∼110 nm) and high entrapment efficiency (∼98%) can be obtained by the reverse micelle–double emulsion method. Results of in vitro experiments show good physical stability and sustained drug release behavior, and a core-shell (mixed micelles enriched core) pattern was confirmed by fluorescence spectra and PAGE. And this novel strategy reported here might be attractive to the development of sustained drug release systems of biological macromolecules for non-parenteral administration.

References

Barichello, J.M., Morishita, M., Takayama, K., Nagai, T., 1999. Absorption of Insulin from Pluronic F-127 gels following subcutaneous administration in rats. Int. J. Pharm. 184, 189–198.

Çilek, A., Çelebi, N., Tırnaksız, F., Tayb, A., 2005. A phospholipid-based microemulsion of rh-insulin with aprotinin for oral administration: Investigation of hypoglycemic effects in non-diabetic and STZ-induced diabetic rats. Int. J. Pharm. 298, 176–185.

Cortesi, R., Esposito, E., Luca, G., Nastruzzi, C., 2002. Production of lipospheres as carriers for bioactive compounds. Biomaterials 23, 2283–2294.

Cui, F.D., Shi, K., Zhang, L.Q., Tao, A.J., Kawashima, Y., 2006. Biodegradable nanoparticles loaded with insulin–phospholipid complex for oral delivery: Preparation, in vitro characterization and in vivo evaluation. J. Control. Release 114, 242–250.

Dubes, A., Lopez, H.P., Abdelwahed, W., Degobert, G., Fessi, H., Shahgaldian, P., Coleman, A.W., 2003. Scanning electron microscopy and atomic force microscopy imaging of solid lipid nanoparticles derived from amphiphilic cyclodextrins. Eur. J. Pharm. Biopharm. 55, 279–282.

Freitas, C., Müller, R.H., 1999. Correlation between long-term stability of solid lipid nanoparticles (SLN^{TM}) and crystallinity of the lipid phase. Eur. J. Pharm. Biopharm. 47, 125–132.

Fuentes, M.G., Torres, D., Alonso, M.J., 2002. Design of lipid nanoparticles for the oral delivery of hydrophilic macromolecules. Colloid Surf. B 27, 159–168.

Fuentes, M.G., Alonso, M.J., Torres, D., 2005. Design and characterization of a new drug nanocarrier made from solid–liquid lipid mixtures. Colloid Surf. 285, 590–598.

Gómez-Pérez, F.J., Rull, J.A., 2005. Insulin therapy: current alternatives. Arch. Med. Res. 36, 258–272.

Hammad, M.A., Müller, B.W., 1998. Increasing drug solubility by means of bile salt-phosphatidylcholine-based mixed micelles. Eur. J. Pharm. Biopharm. 46, 361–367.

Hu, F.Q., Jiang, S.P., Du, Y.Z., Yuan, H., Ye, Y.Q., Zeng, S., 2005. Preparation and characterization of stearic acid nanostructured lipid carriers by solvent diffusion method in an aqueous system. Colloid Surf. B 45, 167–173.

Hunter, R.J., 1987. Foundations of Colloid Science, vol. 1. Calderon Press, Oxford, pp. 228–315.

Komatsu, H., Kitajima, A., Okada, S., 1995. Pharmaceutical characterzation of commercially available intravenous fat emulsions:estimation of average particle size, size distribution and surface potential using photon correlation spectroscopy. Chem. Pharm. Bull. 43, 1412–1415.

Makino, K., Yamamoto, N., Higuchi, K., Harada, N., Ohshima, H., Terada, H., 2003. Phagocytic uptake of polystyrene microspheres by alveolar macrophages: effects of the size and surface properties of the microspheres. Colloid Surf. B 27, 33–39.

Mehnert, W., Mäder, K., 2001. Solid lipid nanoparticles–production, characterization and applications. Adv. Drug Deliv. Rev. 47, 165–196.

Mei, Z.N., Chen, H.B., Weng, T., Yang, Y.J., Yang, X.L., 2003. Solid lipid nanoparticle and microemulsion for topical delivery of triptolide. Eur. J. Pharm. Biopharm. 56, 189–196.

Morel, S., Terreno, E., Ugazio, E., Aime, S., Gasco, M.R., 1998. NMR relaxometric investigations of solid lipid nanoparticles (SLN) containing gadolinium(III) complexes. Eur. J. Pharm. Biopharm. 45, 157–163.

Mühlen, Z., 1996. Feste Lipid Nanopartikel mit prolongierter Wirkstoffliberation. Herstellung, Langzeitstabilität, Charakterisierung, Freisetzungsverhalten und -mechanismen. Ph.D. Thesis. Freie Universität Berlin, Germany.

Müller, R.H., Rühl, D., Runge, S., Schulze-Forster, K., Wolfgang, M., 1997. Cytotoxicity of solid lipid nanoparticles as a function of the lipid matrix and the surfactant. Pharm. Res. 14, 458–462.

Müller, R.H., Jacobs, C., Kayser, O., 2001. Nanosuspensions as particulate drug formulations in therapy: rationale for development and what we can expect for the future. Adv. Drug Deliv. Rev. 47, 3–19.

Müller, R.H., Keck, C.M., 2004. Challenges and solutions for the delivery of biotech drugs—a review of drug nanocrystal technology and lipid nanoparticles. J. Biotechnol. 113, 151–170.

Müller, R.H., Mäder, K., Gohla, S., 2000. Solid lipid nanoparticles (SLN) for controlled drug delivery—a review of the state of the art. Eur. J. Pharm. Biopharm. 50, 161–177.

Müller, R.H., Rühl, D., Runge, S.A., 1996. Biodegradation of solid lipid nanoparticles as a function of lipase incubation time. Int. J. Pharm. 144, 115–121.

Perez, C., Castellanos, I.J., Costantino, H.R., 2002. Recent trends in stabilizing protein structure upon encapsulation and release from biodegradable polymers. J. Pharm. Pharmacol. 54, 301–313.

Pillai, O., Panchagnula, R., 2001. Insulin therapies—past, present and future. Drug Discov. Today 6, 1056–1061.

Schurch, S., Gehr, P., Im Hof, V., Geiser, M., Green, F., 1990. Surfactant displaces particles toward the epithelium in airways and alveoli. Respir. Physiol. 80, 17–32.

Siekmann, B., 1994. Untersuchungen zur Herstellung und zum Rekristallisationsverhalten schmelzemulgierter intravenös applizierbarer Glyceridnanopartikel. Ph.D. Thesis. Technical University of Braunschweig, Germany.

Siekmann, B., Westesen, K., 1992. Submicron-sized parenteral carrier systems based on solid lipids. Pharm. Pharmacol. Lett. 1, 123–126.

Siekmann, B., Westesen, K., 1994b. Thermoanalysis of the recrystallization process of melt-homogenized glyceride nanoparticles. Colloid Surf. B 3, 159–175.

Smith, A., Hunneyball, I.M., 1986. Evaluation of polylactid as a biodegradable drug delivery system for parenteral administration. Int. J. Pharm. 30, 215–230.

Sznitowska, M., Gajewska, M., Janicki, S., Radwanska, A., Lukowski, G., 2001. Bioavailability of diazepam from aqueous-organic solution, submicron emulsion and solid lipid nanoparticles after rectal administration in rabbits. Eur. J. Pharm. Biopharm. 52, 159–163.

Trehan, A., Agsar, A., 1998. Recent approaches in insulin delivery. Drug Dev. Ind. Pharm. 24, 589–597.

Wang, J.X., Sun, X., Zhang, Z.R., 2002. Enhanced brain targeting by synthesis of 3′, 5′-dioctanoyl-5-fluoro-2′-deoxyuridine and incorporation into solid lipid nanoparticles. Eur. J. Pharm. Biopharm. 54, 285–290.

Westesen, K., Bunjes, H., 1995. Do nanoparticles prepared from lipids solid at room temperature always possess a solid lipid matrix? Int. J. Pharm. 115, 129–131.

Westesen, K., Siekmann, B., Koch, M.H.J., 1993. Investigations on the physical state of lipid nanoparticles by synchrotron radiation X-ray diffraction. Int. J. Pharm. 93, 189–199.

Wu, Q.Z., Ping, Q.N., 2003. Study on the structure of insulin stearic acid naniparticles. Chin. Hosp. Pharm. J. 23, 643–645.

Xu, X.L., Fu, Y., Hu, H.Y., Duan, Y.R., Zhang, Z.R., 2006. Quantitative determination of insulin entrapment efficiency in triblock copolymeric nanoparticles by high-performance liquid chromatography. J. Pharm. Biomed. 41, 266–273.

Yamamoto, S., Kobashi, S., Tsutsui, K.I., Yoshimi, S., 2007. Spectroscopic studies of the interaction between methylene blue–naphthol orange complex and anionic and cationic surfactants. Spectrochim. Acta A 66, 302–306.

Yang, S.C., Lu, L.F., Cai, Y., Zhu, J.B., Liang, B.W., Yang, C.Z., 1999. Body distribution in mice of intravenously injected camptothecin solid lipid nanoparticles and targeting effect on brain. J. Control Release 59, 299–307.

Young, T.J., Johnston, K.P., Pace, G.W., Mishra, A.K., 2003. Phospholipid-stabilized Nanoparticles of cyclosporine A by rapid expansion from supercritical to aqueous solution. AAPS Pharm. Sci. Tech., 5, Article 11.

Zhang, K., Wu, X.Y., 2004. Temperature and pH-responsive polymeric composite membranes for controlled delivery of proteins and peptides. Biomaterials 25, 5281–5291.

Zhang, N., Ping, Q.N., Huang, G.H., Xu, W.F., 2005. Investigation of lectin-modified insulin liposomes as carriers for oral administration. Int. J. Pharm. 294, 247–259.